# Solid–liquid transport in a modified co-rotating twin-screw extruder—dynamic simulator and experimental validations

L. Prat [a,*], S. N'Diaye [b], L. Rigal [b], C. Gourdon [a]

[a] *Laboratoire de Génie Chimique–UMR 5503 CNRS, INP-ENSIACET 5, rue Paulin Talabot, BP 1301, 31106 Toulouse Cedex 1, France*

[b] *Laboratoire de Chimie Agroindustrielle–UA INRA 31A1010, INP-ENSIACET, 118 route de Narbonne, 31077 Toulouse Cedex 4, France*

**Abstract**

This work presents a dynamic transport model of a solid–liquid media through a twin-screw extruder (TSE). The application under consideration is the solid–liquid extraction of solute from raw plant substrate. Dynamic experiments are performed and compared with the simulated results for step functions on the solid feed rate and on the screw rotating speed. Despite some imperfections, results allow to validate the simulator.

*Keywords:* Twin-screw extruder; Solid–liquid extraction; Raw plant substrate; Dynamic simulator

## 1. Introduction

An important application domain of twin-screw extruders (TSE) is found in the agro-industry for starch conversion and protein texturisation [1,2]. These contactors allow the simultaneous combination of two unit operations: extrusion and cooking, thus performing both physical and chemical transformations of biopolymers in a single step. TSE can also be used as an extractor, to process essential oils [3], lipids [4], or wood pulping [5,6]. Its ability to carry out extraction and chemical reaction in a single continuous reactor makes TSE very valuable for the valorisation of agroresource wastes [7].

In the setting of solid–liquid extraction from raw plant substrate, twin-screw extruder is considered as a multifunction thermo-mechano-chemical reactor. This complex device (Fig. 1) is essentially constituted of solid and liquid feeding systems and of a variable speed motor that drags the two screws turning in a barrel. The temperature is regulated with induction belts and cooled by water circulation. Screw profiles are composed at will by the user with transport screw elements (direct pitch screw), with reversed screw elements (RSE) and with kneading elements (MAL) with different shapes and functions [8]. Twin-screw extruder is mainly used for its capacity of transfer whatever the viscosity of products and the very large range of mechanical actions that it can exercise on the matter (shearing, bruising, compression, . . . ).

In order to facilitate the clarification of processes in the extruder, it is necessary to be able to develop some fast and sure methods to appraise parameters intervening in transport phenomena, in heat transfer and in mechanical effects within the device. Besides, in order to conduct the industrial implantation of these processes, the setting up of an efficient and robust supervision system will prove to be necessary. Indeed, the raw plant substrate heterogeneity and the fluctuation of solid feeding rate often leads to unsteady-states and can provoke the mechanical blockages of the system.

The objective of this work is to propose a dynamic simulator of the transport of a polyphasic medium raw plant-solvent in a co-rotative and intermeshing TSE. In the first step, a model will be proposed. This model integrates absorption phenomena of the solvent by the solid, as well as the expression of the solute in the final compression. In the second step, experiences will be presented in order to validate the dynamic simulator.

* Corresponding author.
*E-mail address:* laurent.prat@ensiacet.fr (L. Prat).

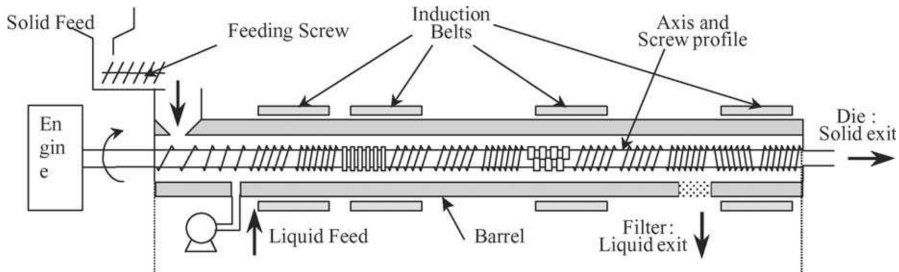


| Type | T2F | C2F | C2F | C2F | Mal2 | C2F | C2F | C2F | Mal0 | C2F | C2F | C2F | CF2C | C2F |
|---|---|---|---|---|---|---|---|---|---|---|---|---|---|---|
| Pitch (mm) | 66 | 50 | 33 | 25 | | 33 | 33 | 25 | | 33 | 33 | 25 | | 25 |
| Length (mm) | 100 | 100 | 100 | 100 | 100 | 100 | 100 | 100 | 100 | 100 | 100 | 100 | 100 | 100 |
| Induction | | | Yes | | Yes | | | | Yes | | | | Yes | |

Fig. 1. Twin-screw extruder description.

## 2. Presentation of the dynamic model

However, the current problem, in a certain way, is quit different from previous studies. If TSE hydrodynamics for food or polymer begin to be well known [9–11], the two phase flow constituted by vegetable matter/liquid does not allow to adopt a mechanical approach for now.

Complexity of the phenomena in this process first lies in the complexity of the vegetable matter itself and second in the important coupling between chemical, mechanical and physical phenomena involved. Intrinsic physico-chemical properties classically used in chemical engineering are not easily accessible or are difficult to define for the vegetable matter. Moreover, local mass balances are complex and require drastically simplified hypothesis to be solved. Physical properties of the vegetable matter, like compressibility, are subject to thorough changes. Its internal structure is affected by the progress of the reactive extraction as NaOH breaks it, and by internal moisture occurrence. Chemically spreading, the vegetable matter is also uneasy to define. In fact, only general classes of compounds (cellulose, hemicelluloses, proteins, pectins, lipids, ...) are used. Each class contains biopolymers that can be very different in terms of molar weight, polymerisation degree as well as transport properties (diffusivity), solubility, etc.

Besides, thermo-mechano-chemical processes in twin-screw extruders exhibit use and possibility advantages which become disadvantages for their modelling. If a combination of thermal, mechanical and chemical effects in a same continuous reactor allows the development of a lot of different processes, it also leads to a high phenomena interdependence.

### 2.1. *Model structure and establishment*

The main theoretical difficulty for the establishment of the model lies in the coupling between the particle and intraparticle physico-chemistry of the vegetable matter on the one hand, and the mechanical and transport phenomena on the other hand (Fig. 2). Their links are direct via operation like crushing or compression, as well as, indirect via the residence time and consequently via the reaction or the adsorption process. In addition, an important retroaction of the screw element geometry on the behaviour within the previous elements prevails.

Furthermore, the filling ratio of the different elements evolves in space and in time [8]. Otherwise, the study of a reactor completely closed to the observation presents many difficulties.

As it has been developed by many authors for polymer and food [12–14], the matter transport has been studied via the residence time distribution (RTD) method [15]. Then a transport model has been proposed [16] for the twin-screw extruder used in raw plant substrate fractionation in steady-state. This work tackles the modelling of transport phenomena with a one-dimensional model. The example

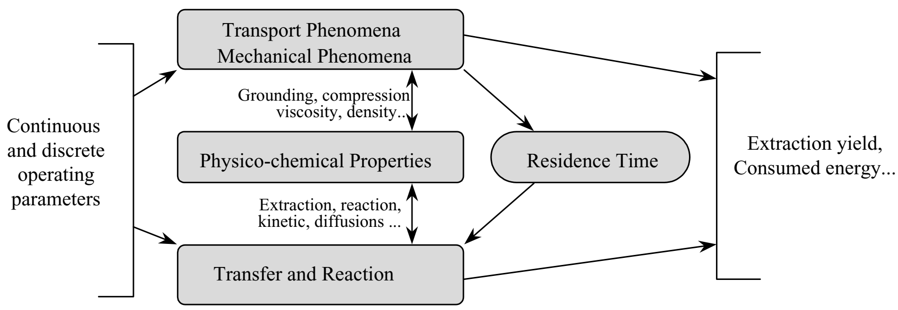


Fig. 2. Phenomena and coupling analysis.

considers the extraction of hemicelluloses from poplar wood with an aqueous solution of sodium carbonate. A screw profile permitting this operation has been finalised [15,17]. This profile includes transport screw elements, kneading elements (which assure the homogeneity of the matter), and reversed screw elements involved in the solid–liquid separation by matter compression over a filter.

The adopted method consists in separating the extruder in functional zones for which a specific model is proposed. These models are based on mass balances and take into account information acquired experimentally in order to integrate knowledge upon the geometry of the different screw elements and on the physico-chemical properties of the solid–liquid substrate. Two categories of screw elements are identified: elements that are always full of matter in steady-state and those that are not. Besides, two zones of the extruder can be differentiated: a zone where the two phases are present, and a zone where the only solid is present (after the filter).

Furthermore, the main process is considered as isothermal. This is mainly due to the presence of water all along the extruder and the low influence of temperature on the matter properties.

### *2.2. Partially filled elements*

Elements of the screw profile that are partially filled are the transport screw to the exception of the one situated upstream of the reversed screw element. It will be considered, in these elements, that there are no phenomena of matter compression (i.e. there is no variation of the solid porosity). Besides, the mass transfer of the liquid phase towards the porous volume of the solid takes place in these elements that are not under mechanical constraints.

The mass balances for solid, liquid and internal liquid phases can be written in an d$x$ length element as follows:

$$\frac{\mathrm{d}m_{\mathrm{S}}}{\mathrm{d}t} = F_{\mathrm{S}} - \frac{Np(1-\alpha)}{\mathrm{d}x} m_{\mathrm{S}} \tag{1}$$

$$\frac{\mathrm{d}m_{\mathrm{L}}}{\mathrm{d}t} = F_{\mathrm{L}} - \frac{Np(1-\alpha)}{\mathrm{d}x} m_{\mathrm{L}} - A \tag{2}$$

$$\frac{\mathrm{d}m_{\mathrm{I}}}{\mathrm{d}t} = F_{\mathrm{I}} - \frac{Np(1-\alpha)}{\mathrm{d}x} m_{\mathrm{I}} + A \tag{3}$$

where $F_{\mathrm{I}}$ is the internal liquid flow entering in an element of volume, from the previous element, $F_{\mathrm{L}}$ the liquid flow entering in an element of volume, from the previous element, $F_{\mathrm{S}}$ the solid flow entering in an element of volume, from the previous element, $m_{\mathrm{I}}$ the internal liquid mass (in the solid porosity) $m_{\mathrm{L}}$ the mass of liquid, $m_{\mathrm{S}}$ the mass of solid, $N$ the screw rotating speed, $p$ the pitch of the transport screw element and $\alpha$ is the factor of shape of the transport element.

The term $A$ is the flux of liquid transferred from the liquid phase toward the porosity of the solid. This global instantaneous flux can be written as:

$$A = K(m_{\mathrm{I\,max}} - m_{\mathrm{I}}) \tag{4}$$

where $m_{\mathrm{I\,max}}$ is the maximal amount of liquid that can be contained by the solid. This term can be expressed with the porosity $\varepsilon$ of the solid, the mass of solid $m_{\mathrm{S}}$ and the ratio of the densities of the liquid and the solid is given by:

$$m_{\mathrm{I\,max}} = \frac{\varepsilon}{1-\varepsilon} \frac{\rho_{\mathrm{L}}}{\rho_{\mathrm{S}}} m_{\mathrm{S}} \tag{5}$$

Finally, on the solid and liquid mass balances it is possible to add a term of mass inlet flow $G$ per unit of time to the corresponding abscissa. In our case, this mass inlet flow appears at the beginning of the TSE (solid feeding zone in the first element and liquid feeding zone in the second element).

### *2.3. Filled elements*

The filled elements of the screw profile are the kneading elements and the RSE. Concerning the transport screw situated upstream of the RSE, previous experiments show that it is filled to the half of its length [8,15]. Indeed, with the solid–liquid system and the processing conditions we used, the pressure drop in the RSE does not seem to have a major influence on the behaviour of the matter in this element. Kneading elements contain the two phases, liquid and solid. The other filled elements are situated after the liquid outlet and then, only the liquid phase is the one contained in the porosity of the solid. The compression of the solid takes place in these elements.

Mass balances for solid and liquid can be expressed in an d$x$ length element by:

$$\frac{\mathrm{d}m_{\mathrm{S}}}{\mathrm{d}t} = F_{\mathrm{S}} - \frac{v_{\mathrm{S}} m_{\mathrm{S}}}{\mathrm{d}x} \tag{6}$$

$$\frac{\mathrm{d}m_{\mathrm{L}}}{\mathrm{d}t} = F_{\mathrm{L}} - \frac{v_{\mathrm{L}} m_{\mathrm{L}}}{\mathrm{d}x} \tag{7}$$

otherwise it is possible to add the two following constraints:

$$\frac{m_{\mathrm{L}}}{\rho_{\mathrm{L}}} + \frac{m_{\mathrm{S}}}{\rho_{\mathrm{S}}} = V \tag{8}$$

$$v_{\mathrm{S}} = \beta v_{\mathrm{L}} \tag{9}$$

as the element is full, it becomes:

$$\frac{\mathrm{d}}{\mathrm{d}t}\left(\frac{m_{\mathrm{S}}}{\rho_{\mathrm{S}}} + \frac{m_{\mathrm{L}}}{\rho_{\mathrm{L}}}\right) = 0 = \frac{F_{\mathrm{S}}}{\rho_{\mathrm{S}}} + \frac{F_{\mathrm{L}}}{\rho_{\mathrm{L}}} - \frac{m_{\mathrm{S}}}{\mathrm{d}x}\frac{\beta v_{\mathrm{L}}}{\rho_{\mathrm{S}}} - \frac{m_{\mathrm{L}}}{\mathrm{d}x}\frac{v_{\mathrm{L}}}{\rho_{\mathrm{L}}} \tag{10}$$

and then

$$\frac{F_{\mathrm{S}}}{\rho_{\mathrm{S}}} + \frac{F_{\mathrm{L}}}{\rho_{\mathrm{L}}} = v_{\mathrm{L}}\left(\frac{m_{\mathrm{S}}}{\mathrm{d}x}\frac{\beta}{\rho_{\mathrm{S}}} + \frac{m_{\mathrm{L}}}{\mathrm{d}x}\frac{1}{\rho_{\mathrm{L}}}\right) \tag{11}$$

so, by using Eqs. (10) and (11) in Eqs. (6) and (7):

$$\frac{\mathrm{d}m_{\mathrm{S}}}{\mathrm{d}t} = F_{\mathrm{S}} - \beta(\rho_{\mathrm{L}} F_{\mathrm{S}} + \rho_{\mathrm{S}} F_{\mathrm{L}}) \frac{m_{\mathrm{S}}}{m_{\mathrm{L}} + \beta m_{\mathrm{S}}} \tag{12}$$

$$\frac{\mathrm{d}m_{\mathrm{L}}}{\mathrm{d}t} = F_{\mathrm{L}} - (\rho_{\mathrm{L}} F_{\mathrm{S}} + \rho_{\mathrm{S}} F_{\mathrm{L}}) \frac{m_{\mathrm{L}}}{m_{\mathrm{L}} + \beta m_{\mathrm{S}}} \tag{13}$$

### 2.4. *Numeric resolution*

Equations are discretised at the second-order in space and the first-order in time. The resolution of the system thus formed is solved with a Runge-Kutta type algorithm.

## 3. Simulations and experimental validations

### 3.1. *Description of the process and the equipment*

The application under consideration is a solid–liquid extraction process of hemicelluloses from poplar wood (populus tremuloïde) via alkaline solubilisation. The used twin-screw extruder is a CLEXTRAL BC45 that includes two co-rotative and intermeshing screws.

Five different kinds of elements are used in the screw profile: T2F (trapezoidal two-flight screw), C2F (two-flight screw), MAL2 (bi-lobe kneading element) always positioned with a $\pi/2$ shift (i.e. in a neutral position for transport compared with conveying screw elements), MAL0 (right-handed mono-lobe kneading element) always positioned with a $\pi/13$ shift (i.e. in a positive position for transport) and C2FC (reversed two-flight screw element). The reverse screw element has peripheral slots grooved in the screw flight for leakage flow. Finally, the pitch of the transport screw elements, varies from 66 to 25 mm. The exact screw profile used is described on Fig. 1.

The ground wood (at an average size of 15 mm × 2 mm × 2 mm) is introduced in head of device by a feeding screw calibrated in mass, at the same time as the liquid phase containing 5% mass in sodium carbonate. A balance permits the registration of the mass in solid outlet (at the die).

### 3.2. *Model parameters*

The considered model requires the knowledge of physico-chemical parameters of the solid and liquid phases (density, porosity), as well as the geometric parameters of the different elements (volume, surface). In the studied case, $\rho_L = 1000\,\mathrm{kg\,m^{-3}}$, $\rho_S = 1220\,\mathrm{kg\,m^{-3}}$, $\varepsilon = 0.78$, and $K = 0.01\,\mathrm{s^{-1}}$. These parameters have been determined independently of the extruder [18].

Finally, the model has an adjustable parameter by type of element of screw:

- The parameter $\alpha$ is for transport screw elements. This parameter characterises the slip velocity of matter in relation to the longitudinal screw velocity.
- The parameter $\beta$ is for the kneading elements. This parameter is the ratio of the solid velocity by the liquid velocity and allows to calculate the mass retention in the screw elements. $\beta$ represents in a global point of view rubbings in kneading elements (i.e. the viscous rubbings and rubbings between matter and barrel).

The values of these adjustable parameter are $\alpha = 0.3$; $\beta_{\mathrm{MAL0}} = 1.42$ (for the MAL0 kneading element) and $\beta_{\mathrm{MAL2}} = 2.05$ (for the MAL2 kneading element). These values have been obtained by parametric identification in steady-state and their physical meaning have been discussed in [16]. In the present paper, the objective is to use these results without changes to predict the dynamics of the system and discuss their accuracy and relevance in that case.

### 3.3. *Experiments*

Once the steady-state is reached, variations are done on the solid feed rate and on the screw rotation velocity. Step functions answers of the system are then measured on the solid instantaneous outlet.

The initial steady-state is obtained with the following values for the operating parameters: screw rotating speed, $N = 2.98\,\mathrm{turns\,s^{-1}}$; liquid feed rate, $Q_L = 5.3\,\mathrm{g\,s^{-1}}$; solid feed rate, $Q_S = 1.09\,\mathrm{g\,s^{-1}}$. Table 1 describes the different variations achieved on $Q_S$ and $N$.

There are three step functions on the solid feed rate and three on the rotating speed screw. The solid phase outlet rate is measured every seconds and is reported in Fig. 3.

### 3.4. *Solid feed rate step function answers*

Fig. 4 describes the answer of the system to a positive and a negative step function on the solid feed rate. Between the two landings in steady-state, the curve presents two dynamic phases separated by a short steady-state.

The first is owed to the change of retention in the kneading element the nearest to the solid outlet, and the second to the kneading element the most distant. Indeed, the reversed screw element and the half transport screw upstream of the RSE remain full because these two elements only contain the solid phase (they are situated after the filter).

Besides, a solid flux change has a direct influence on the liquid flux because of the variations of the internal liquid mass. Indeed, for a liquid flux of $5\,\mathrm{g\,s^{-1}}$, when the solid flux goes from 1 to $2\,\mathrm{g\,s^{-1}}$, the internal liquid quantity grows from 1.5 to $3\,\mathrm{g\,s^{-1}}$ (for a solid weight percentage in the outlet solid $\omega$ of 40%). In steady-state

$$m_I = \frac{1-\omega}{\omega} m_S$$

Table 1
Achieved experiments

| Time (s) | $Q_S$ ($\mathrm{g\,s^{-1}}$) | $N$ ($\mathrm{turns\,s^{-1}}$) |
|---|---|---|
| 0 | 1.09 | 2.98 |
| 290 | 1.9 | |
| 770 | 0.9 | |
| 1380 | | 3.66 |
| 1700 | | 2.98 |
| 1980 | | 3.66 |
| 2160 | 1.9 | |

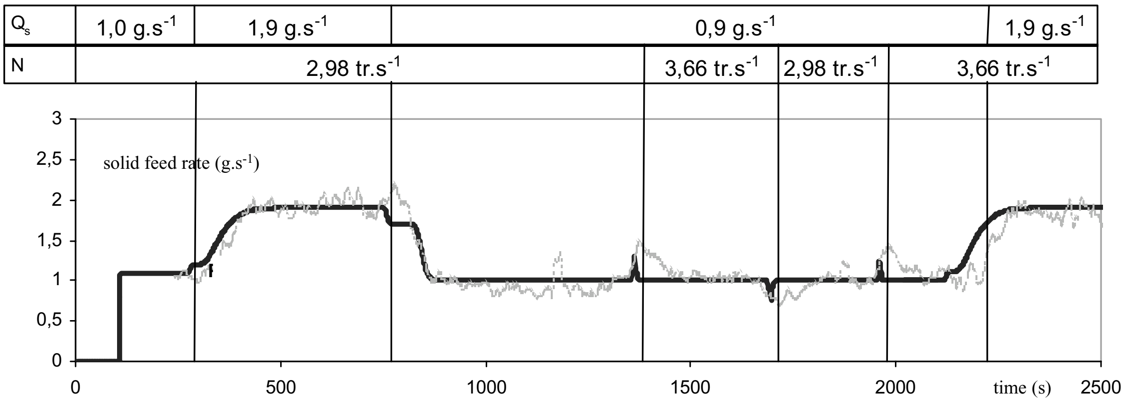


Fig. 3. Model (black line) and experimental (grey line) answers.

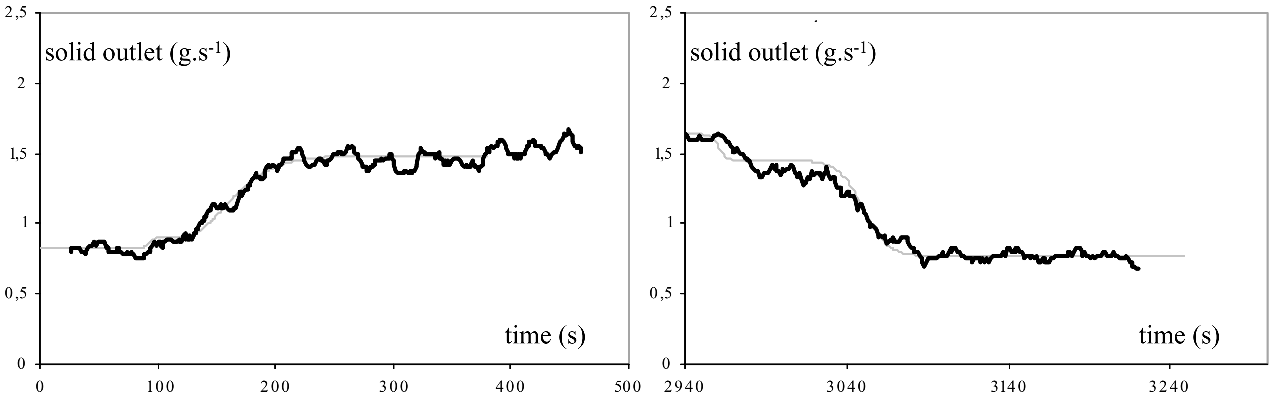


Fig. 4. System answer to step functions on the solid feed rate. Model (grey line) and experimental (black line) answers.

*3.5. Screw rotating speed step function answers*

Fig. 5 describes the answer of the system to a positive followed by a negative step function on the screw rotating speed. The curve presents two peaks separated by a steady-state. The model prediction is not satisfactory. Indeed, according to the model, the variations of rotation speed have only a direct influence on the amount of matter in the transport screws. However, it seems that the rate of compaction in the reversed screw element also depends on this parameter [16]. The model must then be improved in order to better represent the behaviour of this element and then to take into account the dynamic influence on the physical structure on the matter. Of course, this study is far from being easy and will need further improvement on the raw plant knowledge.

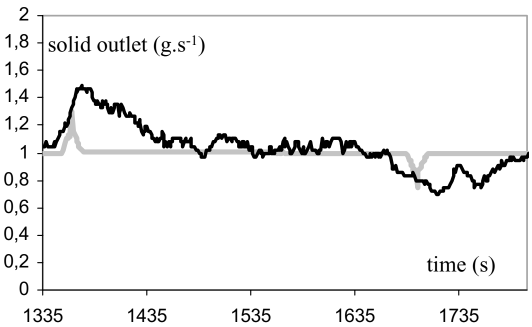


Fig. 5. System answer to step functions on the screw rotating speed. Model (grey line) and experimental (black line) answers.

## 4. Conclusion

The proposed model represents the experimental dynamic results in a correct way in the studied cases. Besides, values of the parameters $\beta_1$ and $\beta_2$ obtained in steady-state by RTD methods are preserved. The coefficient $K$, characterising the apparent global kinetic of transfer of the liquid phase toward the solid did not appear in the steady-state model. Indeed, the time of contact of the two phases in the device is sufficient for the solid to be saturated in liquid at the filter abscissa. Therefore, the influence of this parameter can only be studied in dynamic experiments.

The model must be improved on the reversed screw element to take into account the effect of the rotating speed on the mechanical phenomena. But as far as the considered operation is solid–liquid extraction, the extruder part situated after the filter has less importance.

The proposed model, in spite of its imperfections seems to be adapted to raw plant substrate fractionation in the twin-screw extruder. It can be used to characterise transport phenomena of solid–liquid medium in few experiments and then to avoid fastidious residence time distribution experimental phases. This parameters identification step will, of course, need further study on the mathematical structure as the model sensitivity to the adjustable parameters.

## Acknowledgements

The authors thanks C. Doumeng (CRITT Agroressources–CATAR) for her competence and technical help.

## Appendix A. Nomenclature

- $A$ flux of liquid transferred toward the internal liquid phase
- $F_I$ internal liquid flux entering in an element of volume, from the previous element
- $F_L$ liquid flux entering in an element of volume, from the previous element
- $F_S$ solid flux entering in an element of volume, from the previous element
- $G$ flux of matter entering in an element of volume (feeding)
- $K$ transfer coefficient of the liquid into the solid porosity
- $m_I$ internal liquid mass (in the solid porosity)
- $m_L$ mass of liquid
- $m_S$ mass of solid
- $N$ screw rotating speed
- $p$ pitch of the transport screw element
- $Q_L$ liquid feed rate
- $Q_S$ solid feed rate
- $V$ volume of the mass balance element
- $v_L$ speed of the liquid phase
- $v_S$ speed of the solid phase

*Greek letters*

- $\alpha$ factor of shape of transport element
- $\beta$ ratio of the solid speed by the liquid speed in kneading element
- $\varepsilon$ solid porosity
- $\omega$ solid weight percentage in the solid

## References

[1] J.M. Harper, Food extruders and their applications, in: C. Mercier, P. Linko, J.M. Harper (Eds.), Extrusion Cooking, AACC, St. Paul, MN, 1989, pp. 1–16.
[2] P. Colonna, A. Buleon, Transformations structurales de l'Amidon, in: P. Colonna, G. Della Valle (Eds.), la Cuisson-Extrusion, Lavoisier Tec. et Doc., Paris, 1994, pp. 2–13.
[3] N. Bouzid, G. Villarem, A. Gaset, Extraction des huiles essentielles par des techniques non conventionnelles, Revista Italiana EPPOS, Agosto'97, 1997, pp. 3–11.
[4] S. Isobe, F. Zuber, K. Uemura, A. Nogushi, A new twin-screw press design for oil extraction of dehulled sunflower seeds, J. Am. Oil Chem. Soc. 69 (9) (1992) 884–889.
[5] G. Anon, Procédé et installation de traitement en continu d'une matière cellulosique, French Patent 78 05 495 (1978).
[6] C. De Choudens, R. Angelier, Les pâtes chimicothermomécaniques blanchies obtenues avec le procédé bi-vis, Rev. ATIP 3 (44) (1990) 137–146.
[7] L. Rigal, Technologie d'extrusion bi-vis et fractionnement de la matière végétale, 40 ans d'extrusion bi-vis chez CLEXTRAL, Recueil de conférences, Firminy (France), 8–10 October 1996.
[8] L. Prat, P. Guiraud, L. Rigal, C. Gourdon, Two phase residence time distribution in a modified twin-screw extruder, Chem. Eng. Process. 38 (1999) 73–83.
[9] P. Colonna, J. Tayeb, C. Mercier, B. Vergnes, Flow mixing and residence time distribution of maize starch within a twin-screw extruder with a longitudinally-plit barrel, J. Cereal Sci. 1 (1983) 115–125.
[10] W. Szydlowski, R. Brzoskowski, J.L. White, Modelling flow in an intermeshing corotating twin-screw extruder: flow in kneading discs, Int. Polym. Process. 4 (1998) 207–214.
[11] J. Tayeb, B. Vergnes, G. Della Valle, A basic model for a twin-screw extruder, J. Food Sci. 54 (1989) 1047–1056.
[12] L.P.B.M. Janssen, Twin-Screw Extrusion, Elsevier, Amsterdam, 1978.
[13] R.E. Altamore, P. Ghossi, An analysis of residence time distribution pattern in a twin-screw cooking extruder, Biotechnol. Prog. 2 (3) (1986) 157–163.
[14] P. Boissonat, Etude paramètrique et modélisation des écoulements de la matière par analyse de la distribution des temps de séjour dans trois cuiseurs extrudeurs bi-vis, Doctorat Thesis, Université de Technologie de Compiègne, 1990.
[15] L. Prat, P. Guiraud, C. Gourdon, S. N'Diaye, L. Rigal, Transport d'un milieu complexe polyphasique matériau végétal/solvant en extrudeur bi-vis, 6eme CFGP, 24–26 September 1997, Paris, Récents Progrès en Génie des Procédés, vol. 11, 1997, p. 53.
[16] L. Prat, P. Guiraud, L. Rigal, C. Gourdon, A one dimensional model for the prediction of extraction yields in a two phase modified twin-screw extruder, Chem. Eng. Process. 41 (9) (2002) 743–751.
[17] S. N'Diaye, L. Rigal, P. Laroque, P.F. Vidal, Extraction of hemicelluloses from poplar, populus tremuloides, using an extruder-type twin-screw reactor: influence of the main factors, Bioresour. Technol. 57 (1996) 61–67.
[18] L. Prat, P. Guiraud, L. Rigal, C. Gourdon, Solid–liquid reactive extraction with raw plant substrate, in: Proceedings of the Second European Congress of Chemical Engineering—ECCE 2, Montpellier, France, 5–7 October 1999.